Production of ⁶He, ⁶Li, ⁷Li, and ⁷Be in the $\alpha+a$ reaction between 60—160 MeV

B. G. Glagola

Chemistry Division, Argonne National Laboratory, Argonne, Illinois 60439

V. E. Viola, Jr.

Chemistry Department and Cyclotron Facility, Indiana University, Bloomington, Indiana 47405

H. Breuer, N. S. Chant, A. Nadasen, and P. G. Roos

Physics Department, University of Maryland, College Park, Maryland 20742

Sam M. Austin

Department of Physics and Cyclotron Laboratory, Michigan State University, East Lansing, Michigan 48824

G. J. Mathews

Lawrence Livermore Laboratory, Livermore, California 94550

Cross sections for the production of ⁶He, ⁶Li, ⁷Li, and ⁷Be produced in the $\alpha+\alpha$ reaction have been measured over the energy range 60—160 MeV. Detailed angular distributions are presented for exit channels leading to ⁷Li, ⁷Be, and ⁶Li(g.s.), along with cross sections for the three-body exit channels leading to the production of ⁶He and ⁶Li. The astrophysical significance of the $\alpha+\alpha$ reaction is discussed with particular emphasis on the production of ⁷Li in the interaction of galactic cosmic rays with the interstellar medium. In addition, two-nucleon-transfer distorted-wave Born approximation calculations are presented in an attempt to understand the reaction mechanism operating in the $\alpha(\alpha,d)$⁶Li(g.s.) reaction.

> NUCLEAR REACTIONS ⁴He(⁴He,HI), HI=⁶He, ⁶Li, ⁷Li, and ⁷Be; $E=60$—160 MeV; measured $d^2\sigma/d\Omega\,dE$ and $\sigma(E)$; astrophysical relevance discussed; DWBA calculations for ⁴He(⁴He,d)⁶Li.

I. INTRODUCTION

The $\alpha+\alpha$ reaction is well known to play an important role in the nucleosynthesis of nature's elements.[1] At the sub-Coulomb energies characteristic of stellar interiors, the $\alpha+\alpha\rightarrow$[Be⁸]* reaction provides the critical intermediate step in the 3α reaction which leads to the formation of ¹²C and heavier elements. At higher energies $\alpha+\alpha$ collisions contribute significantly to the abundance of the light element Li via cosmic-ray-like processes. Although the abundance of Li (as well as Be and B) is very low, studies of its origin have important implications on our understanding of the universe.

While big bang nucleosynthesis can account for most of the H and He in the universe[2] and stellar evolution cycles are believed to produce ¹²C and heavier nuclei,[1] the synthesis of Li, Be, and B (Li-

BeB) requires additional mechanisms. Calculations indicate that ⁷Li may be produced in meaningful abundances in the big bang, but the predicted yields for ⁶Li, ⁹Be, ¹⁰B, and ¹¹B are far below the observed values.[2] In the dense, hot environments associated with stellar evolution LiBeB are usually destroyed,[3] which implies that these elements must have their origin in dynamic, nonequilibrium processes. Accordingly, the abundances of LiBeB serve as a valuable indicator of the properties of such phenomena.

One of the most probable mechanisms for production of LiBeB is the interaction of galactic cosmic rays (GCR) with the interstellar medium.[3,4] This mechanism reproduces the measured abundances of ⁶Li, ⁹Be, ¹⁰B, and ¹¹B relatively well. However, attempts to account for ⁷Li via the GCR mechanism result in an underproduction of this

isotope by approximately an order of magnitude, indicating that there must be an additional source of ^{7}Li. The big bang has been suggested as a possible second source of ^{7}Li.[3–6]

In order to evaluate nucleosynthesis models for LiBeB, excitation functions for their production in reactions of the type $\alpha + \alpha$, $p + $CNO, and $\alpha + $CNO (CNO $= ^{12}$C, ^{13}C, ^{14}N, ^{16}O) are required. The energy range must extend from the threshold region to several GeV in order to span the cosmic ray energy spectrum. The $\alpha + \alpha$ reaction requires special consideration as a possible major source of ^{6}Li and ^{7}Li in cosmic ray interactions because this target-projectile pair has by an order of magnitude the highest relative abundance of any other possible combination. Near threshold the $\alpha(\alpha,p)^7$Li and $\alpha(\alpha,n)^7$Be reactions have been studied extensively[5] and the $\alpha(\alpha,d)^6$Li cross sections can be derived from detailed balance calculations.[5,7,8] However, above 50 MeV the available data are sparse with only a few high energy points having been measured.[6,9,10] The present data represent the first systematic determination of the $(\alpha, ^6$Li) and $(\alpha, ^6$He) cross sections over a wide range of energies. In addition, they greatly extend the excitation functions for $A = 6$ and 7 in the $\alpha + \alpha$ reaction necessary for model calculations of LiBeB nucleosynthesis. Preliminary results of these experiments have been previously reported in Ref. 11.

During these experiments elastic scattering cross sections at 160-MeV incident alpha-particle energy were also measured. These data have been reported elsewhere.[12] In order to provide further understanding of the structure and reaction mechanisms of light nuclei, finite-range, two-nucleon transfer DWBA calculations have been undertaken to explain the nature of the ^{6}Li center-of-mass angular distributions resulting from the $\alpha(\alpha,d)^6$Li(g.s.) reaction.

The experimental techniques, data reduction, and results of these measurements are discussed in Secs. II and III. The possible astrophysical implications of these data follow in Sec. IV. The results of the DWBA calculations are presented in Sec. V and finally, a summary of our results is given in Sec. VI.

II. EXPERIMENTAL PROCEDURES

The present experiments were conducted at the University of Maryland 256-cm sector-focused isochronous cyclotron using alpha-particle beams of 61.5, 80.8, 118.9, 139.2 and 158.2 MeV. The optics of the beam-handling system were adjusted to insure a beam energy spread of less than 0.1%. The beam spot size on target was 2 mm $\times$ 2 mm and was checked periodically for stability using a remotely controlled scintillator in the target ladder which could be viewed by a TV camera. Beam intensities ranged from less than 1 to 100 nA depending on the energy and angle of measurement. The charge collected by the Faraday cup mounted downstream from the scattering chamber was monitored by a Tomlinson Model-2000 beam current integrator. The integrated values are known to an accuracy of 2%.[12]

All of the experiments were conducted in a 152-cm-diameter scattering chamber equipped with two remotely-controlled arms which could be positioned to an accuracy of $\pm 0.02°$. The center of the chamber contained a gas target cell and target ladder. The target angle and target height were reproducible to ± 0.1 deg and ± 0.25 mm, respectively. The chamber was sufficiently large to house two ΔE-E telescopes, collimators, and preamps without sacrificing angular resolution or the ability to measure the reaction yields at very small angles. For each energy the absolute zero angle for each telescope was determined from ^{4}He(^{4}He, ^{4}He)^{4}He elastic scattering measurements on both sides of the beam. These data were compared to measurements performed by Frisbee[13] and found to be in good agreement.

The target consisted of a 12.5-cm diameter gas cell designed by Frisbee.[13] For the three highest energies the entrance and exit windows on the gas cell were 11.4 μm thick Havar foil and the ^{4}He gas pressure was 1 atm. Because of the low energy of the heavy reaction products at the two lowest beam energies, a 7.6 μm thick Havar foil exit window and ^{4}He gas pressures near 200 Torr were used in the bombardments. The gas target pressure was monitored continuously during each run with a Wallace Tiernan Series 66A digital differential pressure gauge. The specified accuracy of the gauge is 0.1 Torr.

The primary reaction products of interest in these measurements are ^{6}He, ^{6}Li, ^{7}Li, and ^{7}Be. Of these, ^{7}Li and ^{7}Be result only from two-body final states via (α,p) and (α,n) reactions, respectively. On the other hand, ^{6}Li is produced not only from the two-body (α,d) reaction but also as a three-body final state in the (α,pn) reaction. The nuclide ^{6}He occurs only via the three-body final state $(\alpha,2p)$ reaction.

In order to identify the Z, A, and E of all the heavy products resulting from the above reactions, a triple ΔE-E-VETO silicon semiconductor detector telescope was used. The optimum detector thicknesses for the experiments at the three higher energies were 75 μm, 1 mm, and 4 mm (the latter tilted at an angle of 60° relative to the telescope axis to give an effective thickness of 8 mm), respectively. Because of the low energy of the heavy reaction products in the 61.5- and 80.8-MeV experiments, the triple telescope consisted of detectors in the thicknesses of 23.7 μm, 1 mm, and 1 mm, respectively, with the 1 mm E detector tilted at 45° to the telescope axis to give an effective thickness of 1.4 mm. The combined thickness of detectors ΔE and E was sufficient to stop the most energetic reaction products with $A \geq 6$. The veto detector was used to eliminate the energetic light particles produced in the reaction (primarily elastically scattered alpha particles). When not used in the veto mode, this telescope was used to detect the elastically scattered alpha particles to check the left-right angular symmetry of this telescope and as a monitor for light-ion measurements performed with the second telescope. The collimation system used on this telescope to define the target length in the gas cell and the acceptance solid angle provided an angular resolution of ± 0.2 deg.

As a check on the data collected with the heavy-ion telescope, a second telescope was used to measure the proton production cross section of the $\alpha(\alpha,p)^7$Li reaction. This was a two-element telescope consisting of a 1-mm silicon surface barrier ΔE detector followed by a NaI stopping detector. In the 61.5- and 80.8-MeV experiments the ΔE element of this telescope was 700 μm thick. This telescope was also used as a monitor during the heavy-ion measurements, and to provide data for angles where the kinematics for $A = 6$ and 7 products led to ambiguities in the data. It was found that the proton and ^{7}Li measurements agreed to better than ten percent. The collimators used on this telescope provided an angular resolution of ± 0.4 deg.

Standard electronics were used in these experiments for both telescopes. The systems consisted of a linear amplifier circuit for each detector and standard coincidence requirements; in the case of the heavy-ion telescope a veto circuit was included. The coincidence between each of the detectors in a telescope was used to generate the necessary gate and event triggers. Separate event triggers were used for each telescope. Pulser signals generated at a rate proportional to the beam current were fed to all preamplifiers and analyzed together with the real data in order to monitor gain shifts and dead-time losses in all runs.

III. DATA ANALYSIS AND RESULTS

In these experiments the charge, mass, energy, and angular distributions of the protons and $A \geq 6$ reaction products were measured. Due to the symmetry of the entrance channel for this reaction, the differential cross sections are symmetric about 90° center-of-mass (c.m.). Figure 1 shows an example of the kinematic behavior of the heavy ions in the $\alpha + \alpha$ reaction for an incident alpha-particle energy of 140 MeV. For ^{7}Li and ^{7}Be there are only two particle-stable states: the ground state and the first-excited state (0.477 and 0.429 MeV, respectively). The energy resolution of the experiment was not sufficient to separate these two states for either ^{7}Li or ^{7}Be. The kinematic curves shown for these two nuclei are for the ground state only. The kinematic curve for the ^{6}Li two-body final state is also shown. Since the reactions leading to ^{6}Li and ^{6}He can also result from a three-body final state, the two-body kinematics were calculated for "pseudoexcited states" of the two proton pair plus ^{6}He
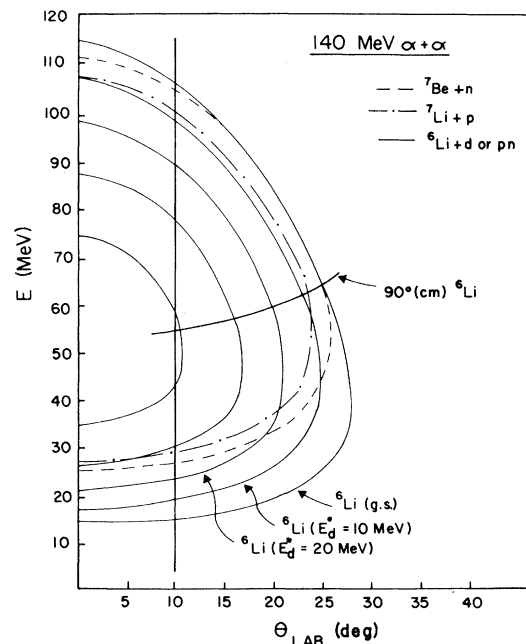

FIG. 1. Heavy-ion two-body final-state kinematic curves in the laboratory system for the $\alpha + \alpha$ reaction at 140-MeV alpha-particle energy.
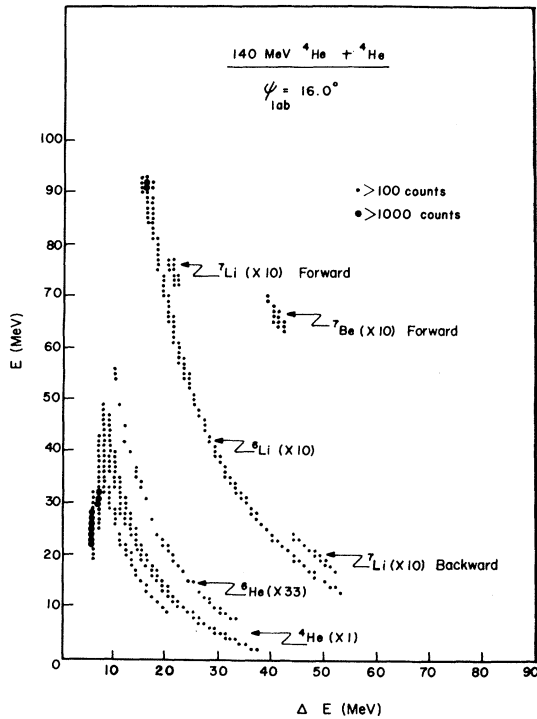
FIG. 2. E-vs-ΔE energy spectrum for the $Z=2-4$ reaction products measured at a laboratory angle of 16° in the 140-MeV $\alpha+\alpha$ experiment.

sional spectrum of E vs ΔE for an incident alpha-particle energy of 140 MeV and heavy ions measured at a lab angle of 16°. It is evident that there is clear identification of the two-body final states, for ^{7}Li from both the forward (c.m.) and backward (c.m.) hemispheres and for ^{7}Be emitted forward. The low energy ^{7}Be emitted in the backward (c.m.) hemisphere was stopped in the ΔE detector in this case, and hence, was not identified. Also shown is the forward two-body final state for ^{6}Li (the most intense high energy ^{6}Li counts), as well as the three-body continuum for ^{6}Li and ^{6}He. As with some of the low energy ^{7}Li and ^{7}Be, it was not possible to obtain the entire ^{6}Li and ^{6}He yields at all angles because of energy loss in the gas target and cell window. Where possible, backward angle (c.m.) data for the two-body final states were extracted to check symmetry about 90° c.m.

The yields $d\sigma/d\Omega$ of the two- and three-body reactions were determined at each angle by integrating the ΔE vs E two-dimensional spectra. (Tables of the differential cross sections for all exit channels are available upon request.) Runs with the target cell evacuated were used to verify that there was no contamination of the spectra due to the gas cell windows. Total production cross sections for the two-body states were calculated by integrating $d\sigma/d\Omega$ in the center-of-mass system. These cross sections are listed in Table I.

Determination of the ^{6}Li three-body final state yields was performed by assuming that the kinematic behavior of these products corresponds to two-body breakup into ^{6}Li and pseudoexcited states of the deuteron. By using the kinematic curves of Fig. 1, the yield of ^{6}Li emitted at angles forward of 90° c.m. could be determined from the energy

and the deuteron plus ^{6}Li. The deuteron pseudoexcited state curves, also shown in Fig. 1, were used in determination of the ^{6}Li continuum cross section, as discussed below.

The angular distributions for all heavy-ion products were measured in steps of 1° or less from 3.5° to 2° beyond the maximum allowable angle in the lab system θ_{max}. Figure 2 shows a two-dimen-

TABLE I. Total production cross sections for the $A=6$ and $A=7$ isotopes in the $\alpha+\alpha$ reaction.

E_α (MeV)	σ(mb)					
	^{6}He (total)	^{6}Li(g.s.)[a]	^{6}Li (cont.)[b]	^{6}Li (total)	^{7}Li[c]	^{7}Be[d]
61.5	1.70±0.21	11.61±0.90	21.66±1.76	33.27±2.31	33.17±2.69	26.80±2.01
80.8	1.93±0.39	7.78±0.52	21.94±1.38	29.72±2.18	16.76±1.08	15.36±1.09
118.9	1.07±0.23	3.11±0.20	18.54±1.10	21.65±1.22	3.99±0.26	3.97±0.25
139.2	0.61±0.15	1.92±0.13	15.74±0.97	17.66±1.04	1.99±0.14	1.99±0.17
158.2	0.37±0.10	1.06±0.06	9.52±0.57	10.58±0.62	0.95±0.08	0.92±0.08

[a] $\alpha(\alpha,d)^6$Li(g.s.) exit channel.
[b] $\alpha(\alpha,pn)^6$Li exit channel.
[c] $\alpha(\alpha,p)^7$Li(g.s + 0.477 MeV).
[d] $\alpha(\alpha,n)^7$Be(g.s. + 0.429 MeV).
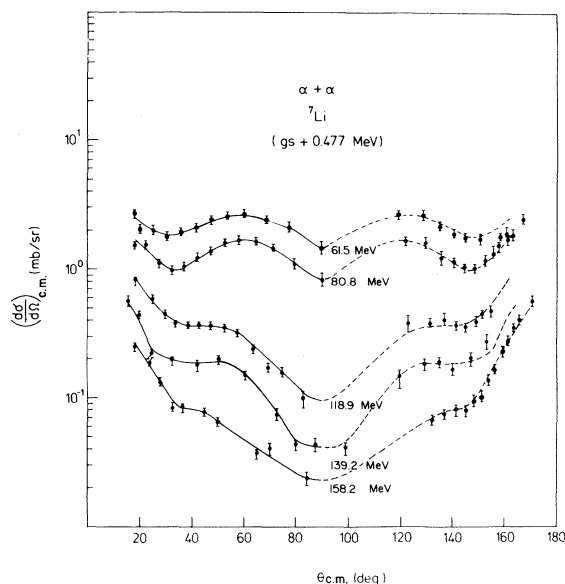
FIG. 3. Center-of-mass angular distributions of ^{7}Li (ground state and first-excited state) from the $\alpha+\alpha$ reaction at alpha-particle energies of $60-160$ MeV. The dashed line is a reflection about 90° c.m. of the solid line (used to guide the eye).

FIG. 5. Center-of-mass angular distributions of ^{6}Li (ground state) from the $\alpha+\alpha$ reaction at alpha-particle energies of $60-160$ MeV. The dashed line is a reflection about 90° c.m. of the solid line (used to guide the eye).

locus corresponding to 90° c.m. for each laboratory angle. This portion of the fragment energy distribution was then integrated to give the forward hemisphere yield and then doubled to obtain the
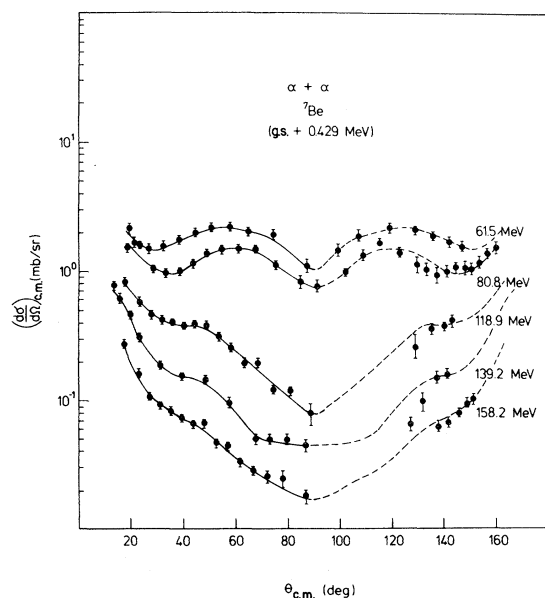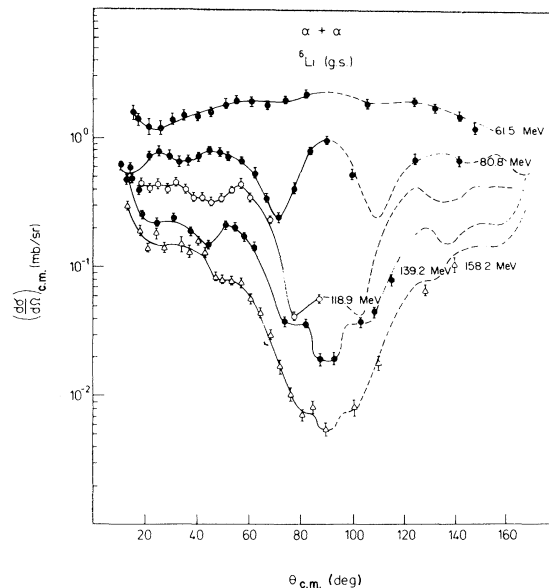

FIG. 4. Center-of-mass angular distributions of ^{7}Be (ground state and first-excited state) from the $\alpha+\alpha$ reaction at alpha-particle energies of $60-160$ MeV.

total yield. A similar procedure was used for the ^{6}He yield. On the basis of comparisons with spectra in which the entire ^{6}Li yield could be observed, the estimated error in this procedure is less than 10%. The total cross sections for both of these reactions were then determined by numerical integration in the laboratory system.

The calculated differential cross sections for the ^{7}Li, ^{7}Be, and ^{6}Li two-body final states are shown in Figs. $3-5$ for all incident alpha-particle energies. The lines drawn in the figures are to guide the eye, with the dashed lines being a reflection of the solid lines about 90° (c.m.). It can be seen from these figures that the angular distributions for ^{7}Be and ^{7}Li are essentially identical. The differential cross sections are rather isotropic at low energies with a slight minimum at 90° and become more forward peaked as the incident alpha-particle energy is increased. These angular distributions suggest that at the higher energies the major contribution to the cross section comes from direct reaction processes. There is also a broad maximum near 60° in the 61.5 MeV data which gradually moves forward in angle and diminishes in magnitude as the incident alpha-particle energy is increased. For the ^{7}Li case there is also a corresponding local maximum in the angular distribution which can be qualitatively understood in terms of a zero-range

PWBA calculation as a p-wave triton transfer to the ^{7}Li ground state.[15] A more realistic accounting of the angular distributions would require consideration of the first excited state as well as inclusion of distortion and finite range effects.

The ^{6}Li ground state angular distribution on the other hand, shows a more radical change in structure as the bombarding energy is increased. The

FIG. 6. Excitation functions for $A=6$ and 7 production in the $\alpha+\alpha$ reaction: (a) ^{7}Be and ^{7}Li (sum of ground state and first-excited state), data below 50 MeV (solid squares) are from Ref. 5 and the solid line is a detailed balance calculation from Ref. 8; above 50 MeV this work (dashed line); (b) ^{6}Li ground state, solid lines based on detailed balance for $(\alpha,d)^6$Li from Refs. 7 and 8. Dashed line from this work, including linear extrapolation to lower energy data or to threshold if no data exist. x-$(\alpha,2p)^6$He reaction; $\Delta(\alpha,pn)^6$Li reaction; ■$(\alpha,d)^6$Li reaction, and ● total ^{6}Li cross section. (c) Comparison of the total $a=6$ cross sections from this work (solid line) with estimates of Refs. 19 (dotted-dashed line) and 16 (dashed line).

distribution is nearly isotropic for the lowest energy. At 80.8 MeV there is a maximum at 90°, with a sharp minimum at about 70°. As the beam energy is increased, the maximum at 90° decreases in intensity until at 158.2 MeV; there is in fact a minimum at 90° and the distributions are strongly peaked toward 0° and 180° (c.m.). These ^{6}Li(g.s.) angular distributions will be discussed further in Sec. V in terms of a two nucleon transfer reaction.

The excitation functions for the various products observed in this reaction are plotted in Fig. 6. It should be noted that the ^{7}Li and ^{7}Be production cross sections shown in Fig. 6(a) are identical to within the limits of error for all energies in the present study and agree well with other measurements at an alpha-particle energy of 103 MeV.[9] In fact, this work clears up a previous discrepancy in the 140-MeV elastic scattering measurements of Refs. 13 and 14. The elastic alpha-particle cross sections measured as a monitor in this experiment agree with the Frisbee[13] measurements. Therefore, it was found that the 140-MeV cross sections of Ref. 14 were high by a factor of about 30%. After removing this factor from the earlier work,[6] the ^{7}Li and ^{7}Be data are found to be in excellent agreement with the present work.

A second feature to be noted about the ^{7}Li and ^{7}Be cross sections is that beyond 60 MeV they undergo an exponential decrease with increasing incident alpha-particle energy. Yiou and Raisbeck[10] have reported cross sections of 0.04, 0.03, and 0.03 mb for ^{7}Be at 400, 600, and 1000 MeV, respectively. Extrapolation of our data to higher energies suggests that this limit is reached near 250−300 MeV. Hence, the present data lead to the conclusion that beyond about 200 MeV, the $\alpha+\alpha$ reaction is a negligible source of ^{7}Li in cosmic-ray-like processes. The measured $A=7$ cross sections are in general agreement with early detailed balance calculations by Mitler[16] and Hayakawa[17] with an extrapolation through the data of Craig et al.[18] at 105 and 112 MeV. However, beyond this energy their calculations overestimate the cross sections by approximately two orders of magnitude.

The mass $A=6$ excitation functions for the various exit channels are presented in Fig. 6(b), along with detailed-balance calculations for the ^{6}Li two-body final state based upon the measurements of Refs. 7 and 8 (the data of Ref. 8 were normalized to those of Ref. 7 in the calculation). The data for the formation of ^{6}Li via the two-body (α,d) reaction are similar to the $A=7$ result beyond the peak

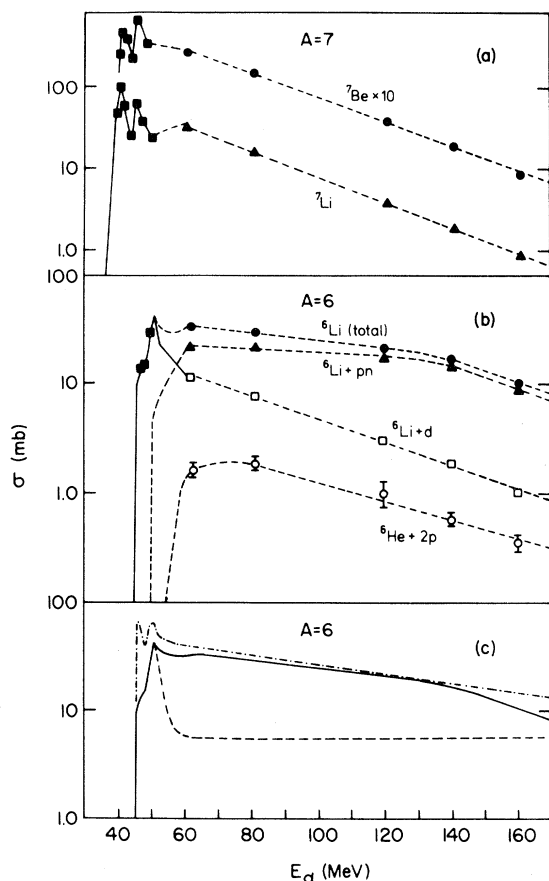near threshold, i.e., the cross sections decrease exponentially with increasing bombarding energy, although the slope is less steep than for $A = 7$. These cross sections agree well with the previously reported data of King *et al.*[6] The previously unmeasured three-body (α,pn) reaction is seen to be essentially constant from above threshold to an energy of approximately $E_\alpha = 140$ MeV. At alpha-particle energies greater than 140 MeV this cross section appears to be decreasing, but it is not clear what the slope of the excitation function is at higher energies. The recent results for total ^{6}Li production in the $\alpha + \alpha$ reaction at 103 MeV reported by Alard *et al.*[9] are about a factor of 2 lower than the results presented here although there is agreement in the $A = 7$ cross sections. One possible explanation of this discrepancy could be that the laboratory angular distribution of Ref. 9 was measured only as far forward as a laboratory angle of 9° and shows a sharp decrease in ^{6}Li cross section at that angle. For the ^{6}Li(g.s.) channel 9° in the laboratory system corresponds to about 30° in the center-of-mass system. Hence, as can be seen in Fig. 7 from comparison of the differential cross sections at 80.9, 103, and 118.9 MeV, respectively, a large fraction of the cross section in this channel could have been missed in Ref. 9. By interpolating the angular distributions from our ^{6}Li data and superimposing these on the data of Ref. 9, the total ^{6}Li cross section at 103 MeV turns out to be in good agreement with the excitation function presented in Fig. 6.

The excitation function for the $\alpha(\alpha,2p)^6$He reaction [Fig. 6(b)] is seen to rise rapidly to a maximum near threshold and then to decrease exponentially with increasing energy. Consequently, above 80 MeV, the dominant contribution to the $A = 6$ cross section is the (α,pn) exit channel. ^{6}Li becomes the dominant heavy reaction product in the $\alpha + \alpha$ reaction for these energies.

In Fig. 6(c) we have compared the measured total $A = 6$ excitation function with estimates of Meneguzzi, Audouze, and Reeves (MAR)[19] and Mitler.[16] It is observed that near threshold the cross sections of MAR overestimate the data by a factor of 2 and that extrapolation to energies beyond 150 MeV leads to cross-section values that are again too high. In contrast, the excitation function of Mitler is seen to underestimate the cross section seriously just beyond threshold. The primary difference is due to the relatively large increase of the ^{6}Li yield due to the (α,pn) reaction channel, which was previously unreported.
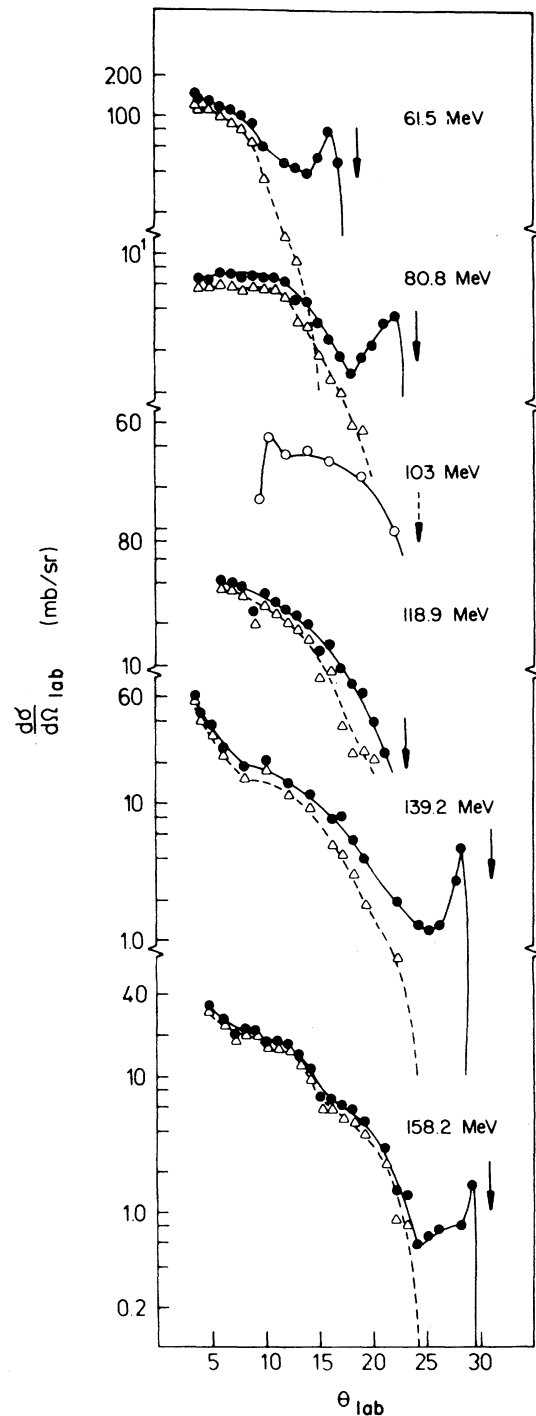

FIG. 7. Laboratory angular distributions for the $\alpha + \alpha \rightarrow d - {}^6$Li (total) reaction. Solid points (●) are for total ^{6}Li from the present work; open points (○) are total ^{6}Li from Ref. 9; the solid lines are to guide the eye; the dashed line and open triangles show the contribution from the $\alpha(\alpha,pn)^6$Li exit channel. The arrows indicate the maximum angle kinematically allowed for ^{6}Li emission.

TABLE II. Total abundances (relative to Si $= 10^6$) and abundance ratios for the light elements produced in interactions between GCR and the interstellar medium ($\Lambda = 5$ g/cm^2). Numbers in parenthesis are error factors. Experimental abundances are from Ref. 23 and calculations from Ref. 26.

	^{6}Li	^{7}Li	^{9}Be	^{10}B	^{11}B
experimental	2.9(1.4)	25(1.4)	0.38(2)	1.1(3)	4.3(3)
calculated	2.6	3.4	0.43	2.1	5.5

	^{7}Li/^{6}Li	^{11}B/^{10}B	^{6}Li/Be	B/^{6}Li
experimental	12.6±0.2	4.05±0.10	5.3(2.3)	2.6(2.7)
calculated	1.31	2.57	6.1	2.9

IV. ASTROPHYSICAL IMPLICATIONS

As stated previously, the GCR mechanism successfully reproduces the observed absolute abundances of the light nuclei ^{6}Li, ^{9}Be, ^{10}B, and ^{11}B within their measured uncertainties, but underproduces ^{7}Li by about a factor of 10. In examining the cosmic abundance ratios for the isotopic pairs, ^{7}Li/^{6}Li and ^{11}B/^{10}B, one finds the calculated GCR ^{11}B/^{10}B ratio is low by about a factor of 2 and the calculated GCR ^{7}Li/^{6}Li ratio is low by a factor of 10, far outside the limits of error. On the other hand, the calculated GCR values for both these ratios agree rather well with the (^{7}Be + ^{7}Li)/^{6}Li and ^{11}B/(^{10}B + ^{10}Be) ratio found in the galactic cosmic ray flux.[20] This latter result provides a strong argument that the GCR mechanism is at least in part responsible for the origin of LiBeB. However, in order to reproduce the observed isotopic ratios, it is clear that a second mechanism is required for both ^{7}Li/^{6}Li and ^{11}B/^{10}B.

As is noted in a recent review by Austin,[21] either destruction of ^{10}B or production of ^{11}B by low-energy particles can remove this difference, with the latter being more probable. This possibility has been examined by several authors.[19,22−24] Even though the addition of a low-energy particle flux [e.g., $\phi(E)\alpha E^{-3}$] can correct the ^{11}B/^{10}B ratio, the model still underestimates the ^{7}Li/^{6}Li ratio by a factor of 4−6. With the addition of the present $\alpha + \alpha$ data and recent $\alpha +$CNO measurements from 40−160 MeV by Gökmen et al.[25] to the existing cross-section data, the determination of all relevant cross sections appears to be complete, except for the true shape of the $\alpha + \alpha \rightarrow A = 6$ excitation function at high energies. Thus, the long-standing underproduction of ^{7}Li persists, as is shown by a recent calculation for LiBeB by Read,[26] which uses these updated cross sections

and various spectral shapes. Table II summarizes this analysis.

Prior to these measurements the $\alpha + \alpha$ reaction was believed to be a possible source of ^{7}Li for the GRC mechanism which might account for the ^{7}Li/^{6}Li ratio of 12.6/1. However, the present data accentuate the discrepancy instead of resolving it. This effect is illustrated in Fig. 8, where we have plotted the ratio of the total cross section for $A = 7$ production to that for $A = 6$ as a function of alpha-particle bombarding energy. As can be seen, the present data lead to the conclusion that beyond about 200 MeV, the $\alpha + \alpha$ reaction is a negligible source of ^{7}Li in the galactic cosmic ray context. This figure also illustrates the fact that the $\alpha + \alpha$ reaction cannot be used to remove the discrepancy between the calculated and observed ^{7}Li/^{6}Li ratio. Indeed, if instead of extrapolating the $A = 6$ cross section with an exponential fall off to high energies, one assumes that the cross section remains constant at the 140 MeV values, the resulting ^{7}Li/^{6}Li ratio from the $\alpha + \alpha$ reaction is even lower (as seen by the dashed line in Fig. 8). The true behavior of the ^{7}Li/^{6}Li cross section ratio probably lies between these two assumptions. This fact adds additional support to the idea that a second source of ^{7}Li production is still needed.

Since ^{7}Li is also produced in the big bang,[4] it has been argued by many authors that this may be the additional source of ^{7}Li. In fact, the assumption that the big bang does not produce more ^{7}Li than is presently observed leads to limits on the baryon density of the universe. By using the standard big bang calculations,[27−29] one finds that an inferred mean baryon density of $\rho \sim 5 - 9 \times 10^{-31}$ g/cm^3 is consistent with the residual ^{7}Li abundance. This value is consistent with the baryon density derived from the deuterium abundance.[30] This type of calculation, however,
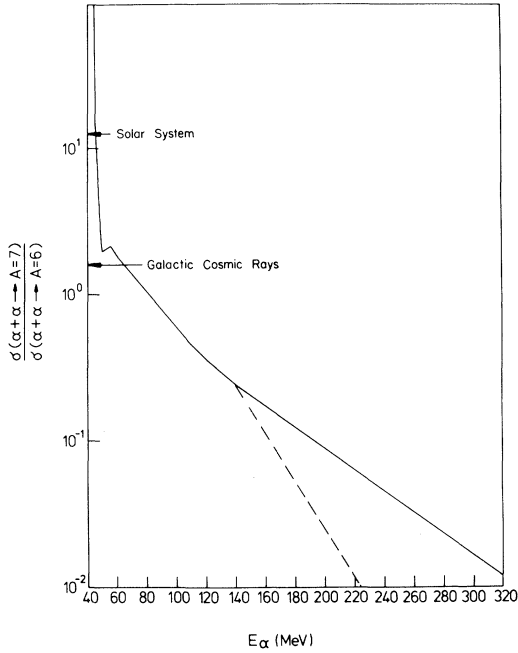
FIG. 8. Ratio of the cross sections for mass 7 to mass 6 production in the $\alpha+\alpha$ reaction versus incident alpha-particle energy.

does not include the effects of infall and astration on the ^{7}Li abundance. Mathews and Viola[31] have pointed out that a comparison of the experimental and calculated values of the ratio $X(^2H)/X(^7\text{Li})$ provides an estimate of the baryon density insensitive to the effects of astration. The value of ρ_B

obtained in this manner is in good agreement with previous results and supports the conclusion that the universe is open. A detailed review of this problem has recently been given by Austin.[21]

These data are also relevant to several other problems in nuclear astrophysics. The $\alpha+\alpha$ reaction can be used to evaluate possible galactic production of deuterium and ^{7}Li. The situation is not yet so clear for the case of ^{6}Li. If one assumes that the mass 6 cross section decreases exponentially beyond 140 MeV, as indicated by the 160 MeV point, then the predicted ^{6}Li abundance is in good agreement with that observed, as shown in Table II. If on the other hand it is assumed that the cross section remains constant beyond 160 MeV, the abundance is over-predicted in the GCR model. Measurements of $\alpha+\alpha\rightarrow$ mass 6 at higher energies will be needed to resolve this ambiguity. The more detailed ^{7}Li and ^{7}Be excitation functions that now exist can be used to refine calculations[32] of the probability of observing gamma-ray lines from the $\alpha+\alpha$ reaction and possibly setting limits on the present rate of production of ^{7}Li in the galaxy. Finally, these data are useful in evaluating additional sources of ^{7}Li, e.g., flare regions, surfaces of neutron stars[33] and carbon stars.[34]

V. DWBA CALCULATIONS

To understand the angular distributions of the $\alpha(\alpha,d)^6$Li reaction, two-nucleon-transfer DWBA calculations were carried out using the exact

TABLE III. Potential parameters used in the DWBA calculations.

	$\alpha+\alpha^a$	$d+^6\text{Li}^b$	10 MeV $d+^6\text{Li}^c$	
r_0	0.151	1.050	2.17	
a_0	1.059	0.783	0.61	
r_w	2.169	1.280	2.35	
a_w	0.362	0.746	0.25	
W_D		8.63 MeV	20.4	
E_{lab}	V (MeV)	W_V (MeV)	V (MeV)	V (MeV)
61.5	304.6	7.78	100.3	95.9
80.8	298.3	8.80	95.3	
118.9	285.7	10.83	85.3	
139.2	279.4	11.84	80.3	
158.2	273.2	12.86	75.3	

[a]From Ref. 12.
[b]Set II potentials from Ref. 37.
[c]From Ref. 38.

finite-range code MARY2,[35] which utilizes a multipole expansion of the range function

$$D(\vec{r},\vec{s}) = \int \phi_d(r_{34})\vec{V}_{10}\phi_\alpha(\vec{r}_{34}\vec{r},\vec{s})d\vec{r}_{34} .$$

The functions ϕ_α and ϕ_d are the internal wave functions[36] for the α and d, respectively, and $\vec{V}_{10}$ is the sum of spin-averaged nucleon-nucleon interactions between the deuteron and the transferred particles.

Since the incoming channel consists of identical α particles, the transition amplitude was symmetrized. Thus the cross section is given by

$$\frac{d\sigma}{d\Omega} \propto |f(\theta)+f(\pi-\theta)|^2$$

instead of $|f(\theta)|^2$.

The $\alpha+\alpha$ distorting potentials were derived from the work of Nadasen et al.,[12] while the $d+^6$Li potentials were obtained from the energy-dependent analyses of Hinterberger et al.[37] The potential parameters used at the various energies are listed in Table III.

The angular distributions of both the data and the DWBA calculations (solid lines) along with the spectroscopic factors are shown in Fig. 9. Except for 60 MeV, the shapes of the angular distributions are qualitatively reproduced by the calculations. The extracted spectroscopic factors (ranging from 0.49 at 60 MeV to 0.30 at 160 MeV) are very reasonable in that they remain almost constant in going from 60 to 160 MeV and are close to the theoretically expected value of 1.0.

The 60-MeV data, and to some extent the 80-MeV data, seem to be much more isotropic than the calculations would predict. Since the Q value for this reaction is -22.4 MeV, the center-of-mass energy for the outgoing $d+^6$Li channel at 60 MeV bombarding energy is only 7.6 MeV. It is, therefore, questionable whether the extrapolation of Hinterberger's parameters to such a low energy is reliable. In view of this uncertainty, calculations were made with published[38] 10-MeV $d+^6$Li parameters. These results are shown as the dashed line in Fig. 9 normalized by a factor of 0.49 and seem to be much closer to the shape of the data. The more isotropic behavior of the data relative to the calculations is not surprising because at such a low energy, compound nucleus formation due to d-^{6}Li resonances are expected to dominate the reaction. This would add an isotropic background, which is not included in the DWBA calculations, and thus may explain the discrepancy between calculations and data.
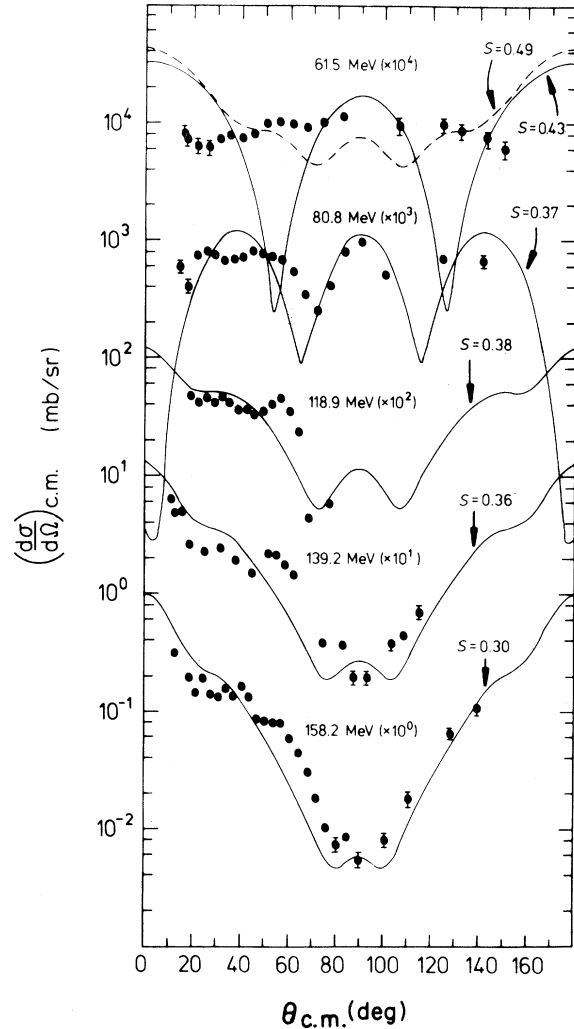

FIG. 9. Comparison of the two-nucleon-transfer DWBA calculations of the $\alpha(\alpha,d)^6$Li(g.s.) center-of-mass angular distributions to the experimental data points. The solid curves are obtained using the energy-dependent $d+^6$Li potentials derived from Ref. 38. The spectroscopic factor for each energy is also shown.

An attempt to extrapolate the 10-MeV potentials (using Hinterberger's energy dependence) for calculations of the 80-MeV data proved unsuccessful. This further reflects the uncertainty of the energy dependence at these low energies. Nevertheless, contributions from compound systems cannot be ruled out even for the 80-MeV data.

It thus seems appropriate to conclude that the higher energy data could be described by a direct two-nucleon-transfer reaction mechanism. For the two lowest energies other processes such as decay from compound systems appear to contribute significantly to the measured cross section.

VI. CONCLUSIONS

We have measured angular distributions and total cross sections for the production of ^{6}He, ^{6}Li, ^{7}Li, and ^{7}Be from the $\alpha+\alpha$ reaction over the energy range of 60 MeV $< E_\alpha < 160$ MeV. The angular distributions evolve from nearly isotropic character at 60 MeV to strongly forward-peaked at 160 MeV. The total $A = 7$ cross sections are found to decrease nearly exponentially over this energy range while those for $A = 6$ remain rather constant or decrease slowly, largely due to influence of the (α, pn) reaction.

The $\alpha+\alpha$ reaction is astrophysically significant in evaluating production mechanisms for the nuclides ^{6}Li and ^{7}Li in a variety of cosmological settings. The addition of the present data to the $\alpha+\alpha$ excitation functions confirms that this reaction is not a significant source of ^{7}Li in the galactic cosmic ray context. Whether the GCR calculation properly reproduces the ^{6}Li abundance depends on the behavior of the $\alpha+\alpha\rightarrow$mass 6 cross section above the measured energy range; i.e., whether it remains constant or decreases. Hence, now that all of the salient reaction cross sections have been measured (p +CNO, α +CNO, and $\alpha+\alpha$), one is left with the conclusion that the GCR mechanism underproduces ^{7}Li by approximately an order of magnitude and an additional source(s) is required. One very plausible source of ^{7}Li is the big bang. Determinations of the universal baryon density based on big bang production of the additional ^{7}Li is consistent with the baryon density derived from the deuterium abundance, and supports the conclusion that the universe is open.

We have also presented calculations using a two-nucleon-transfer DWBA code in an attempt to understand the mechanism of the $\alpha(\alpha,d)^6$Li(g.s.) reaction. At the higher energies this mechanism describes the data quite well. However, at lower energies the data are more isotropic than the calculations predict and appear to indicate that a second mechanism such as compound nucleus formation is also operating.

[1]E. M. Burbidge, G. R. Burbidge, W. A. Fowler, and F. Hoyle, Rev. Mod. Phys. 29, 547 (1957); see also V. Trimble, *ibid.* 47, 877 (1075).

[2]H. Reeves, J. Audouze, W. A. Fowler, and D. N. Schramm, Astrophys. J. 179, 909 (1973).

[3]H. Reeves, Annu. Rev. Astron. Astrophys. 12, 437 (1974).

[4]D. N. Schramm and R. V. Wagoner, Annu. Rev. Nucl. Sci. 27, 37 (1977).

[5]C. H. King, S. M. Austin, H. H. Rossner, and W. H. Chien, Phys. Rev. C 16, 1712 (1977).

[6]C. H. King, H. H. Rossner, S. M. Austin, W. S. Chien, G. J. Mathews, V. E. Viola, Jr., and R. G. Clark, Phys. Rev. Lett. 35, 988 (1975).

[7]C. R. Mclenahan and R. E. Segal, Phys. Rev. C 11, 370 (1975).

[8]J. M. F. Jeronymo, G. S. Mani, F. Picard, and A. Sadeghi, Nucl. Phys. 38, 11 (1962); G. S. Mani, R. M. Freeman, F. Picard, D. Redon, and A. Sadeghi, Proc. Phys. Soc. London 85, 281 (1965).

[9]J. P. Alard, M. M. Avomenze, J. P. Costilhes, J. Fargeix, and G. Roche, Nucl. Instrum. Methods 160, 419 (1979).

[10]F. Yiou and G. M. Raisbeck, *Proceedings of the 15th International Cosmic Ray Conference, Plovdv, 1977,* edited by B. Betev (Bulgarian Academy of Sciences, Sofia, 1977), p. 133.

[11]B. G. Glagola, G. J. Mathews, H. F. Breuer, V. E. Viola, P. G. Roos, A. Nadasen, and Sam M. Austin, Phys. Rev. Lett. 41, 1698 (1979).

[12]A. Nadasen, P. G. Roos, B. G. Glagola, G. J. Mathews, V. E. Viola, Jr., H. G. Pugh, and P. Frisbee, Phys. Rev. C 18, 2792 (1978).

[13]P. E. Frisbee, Ph.D. thesis, University of Maryland, 1972 (unpublished).

[14]G. J. Mathews, Ph.D. thesis, University of Maryland, 1977 (unpublished).

[15]D. W. Devins, S. M. Bunch, H. H. Forster, J. Kokhikian, and C. C. Kim, Nucl. Phys. A126, 261 (1969).

[16]H. E. Mitler, Astrophys. Space Sci. <u>17</u>, 186 (1972).

[17]S. Hayakawa, Prog. Theor. Phys. (Japan), Suppl. <u>40</u>, 156 (1968).

[18]R. M. Craig, B. Hird, C. J. Kost, and T. Y. Li, Nucl. Phys. <u>A96</u>, 367 (1967).

[19]M. Meneguzzi, J. Audouze, and H. Reeves, Astron. Astrophys. <u>15</u>, 337 (1971).

[20]N. J. Westergaard, Astrophys. J. <u>233</u>, <u>374</u>, (1979).

[21]S. M. Austin, Prog. Part. Nucl. Phys. <u>40</u>, 14 (1980).

[22]D. Bodansky, W. W. Jacobs, and D. L. Oberg, Astrophys. J. <u>202</u>, 222 (1975).

[23]H. Reeves and J.-P. Meyer, Astrophys. J. <u>226</u>, 613 (1978).

[24]R. A. Moyle, B. G. Glagola, G. J. Mathews, and V. E. Viola, Phys. Rev. C <u>19</u>, 631 (1979).

[25]A. Gökmen, H. Breuer, B. G. Glagola, and V. E. Viola, Indiana Nuclear Chemistry Report INC-40007-8 (unpublished).

[26]S. M. Read and V. E. Viola, Indiana Nuclear Chemistry Report INC-40007-3, 1981 (unpublished).

[27]R. V. Wagoner, Astrophys. J. <u>179</u>, 343 (1973).

[28]S. M. Austin and C. H. King, Nature <u>269</u>, 782 (1977).

[29]G. Beaudet and A. Yahil, Astrophys. J. <u>218</u>, 253 (1977).

[30]J. R. Gott, J. E. Gunn, D. N. Schramm, and B. M. Tinsley, Astrophys. J. <u>194</u>, 543 (1974).

[31]G. J. Mathews and V. E. Viola, Jr., Astrophys. J. <u>228</u>, 375 (1979).

[32]B. Kozlovsky and R. Ramaty, Astrophys. Lett. <u>19</u>, 19 (1977).

[33]D. D. Clayton and E. Dwek, Astrophys. J. <u>206</u>, L59 (1976).

[34]R. Canal, J. Isern, and B. Sanahuja, Astrophys. J. <u>220</u>, 606 (1978).

[35]N. S. Chant, Nucl. Phys. <u>A211</u>, 269 (1973).

[36]N. Frascaria, J. P. Didelez, N. S. Chant, and C. C. Chang, Phys. Rev. C <u>16</u>, 603 (1977).

[37]F. Hinterberger, G. Mairle, U. Schmidt-Rohr, G. J. Wagner, and P. Turek, Nucl. Phys. <u>A111</u>, 265 (1968).

[38]H. G. Bingham, A. R. Zander, K. W. Kemper, and N. R. Fletcher, Nucl. Phys. <u>A173</u>, 265 (1971).